

RESEARCH ARTICLE



Isothermal Modelling of Glyphosate Herbicide Adsorption Using Biochar and Humic Substances from Palm Oil Mill Waste

Salma Athiyya^a, Yulnafatmawita^b, Amsar Maulana^c, Herviyanti^b

^a Master Program of Soil Science, Agriculture Faculty, Andalas University, Limau Manis, Padang City, 35141, Indonesia

^b Department of Soil Science and Land Resources, Agriculture Faculty, Andalas University, Limau Manis, Padang City, 35141, Indonesia

^c Post-Doctoral Program of Agriculture Faculty, Andalas University, Limau Manis, Padang City, 35141, Indonesia

Article History

Received

11 September 2025

Revised

28 September 2025

Accepted 16 October 2025

Keywords

adsorption isotherm,
glyphosate, palm oil mill
waste



ABSTRACT

The increasing use of glyphosate containing herbicides raises environmental concerns. These herbicides are persistent environmental pollutants and may harm soil and aquatic ecosystems. Although previous studies have evaluated different adsorbents, the use of palm oil mill waste for glyphosate containment has not been thoroughly researched. This study attempts to fill this gap by turning palm oil mill waste into eco-friendly adsorbents: biochar and humic substances. This study seeks to identify the glyphosate adsorption characteristics of diverse palm oil waste formulations in order to determine the optimal formulation through an isothermal adsorption analysis. Two major materials were used in the batch equilibrium experiments: biochar created from empty palm fruit bunches (B-OPEFB) and humic substances derived from wet decanter solids (HS-WDS). Each of these adsorbents were used on their own, and in different combinations to test how well they retained glyphosate. The results revealed that the adsorption capacity of biochar is largely due to its carbon-porous matrix, while humic substances contribute to the adsorption via chemical interactions that are facilitated by active functional groups. Out of all the combinations, the one containing 25% biochar and 75% humic substances achieved the best adsorption efficiencies. The adsorption behavior of this combination was best described by the Langmuir isotherm, with a strong correlation ($R^2 > 0.97$). This clearly demonstrates the effectiveness of waste palm oil mills as a soil amendment to reduce glyphosate contamination. In addition, this waste transformation to active materials for environmental protection supports the practice of sustainable agriculture.

Introduction

Glyphosate [N-(*phosphonomethyl*) glycine] is one of the most widely applied herbicides in global agriculture due to its effectiveness in controlling a broad spectrum of weeds. However, its extensive and repetitive use has led to increasing environmental concerns, particularly related to its persistence in soil and water systems, potential toxicity to non-target organisms [1], and disruption of microbial communities [2]. Glyphosate is known to have a high affinity for soil components; however, under certain conditions, it can become mobile and leach into groundwater, contributing to broader ecological risks. Several adsorbents have been tested for their ability to retain glyphosate, including activated carbon, clay minerals, ion-exchange resins, zeolites, biochar produced from different feedstocks, and more recently, metal-organic frameworks (MOFs). Activated carbon [3] is well known for its very large surface area and microporous structure, which provides strong sorption sites; nevertheless, its relatively high production cost and tendency for pore blockage during repeated use limit its practical application.

Clay minerals [4] such as kaolinite and montmorillonite, also show affinity for glyphosate through their negatively charged surfaces; however, their capacity is highly dependent on soil pH and the presence of competing cations, which makes their performance less predictable under field conditions. Ion-exchange

Corresponding Author: Herviyanti



herviyanti@agr.unand.ac.id



Department of Soil Science and Land Resources, Agriculture Faculty, Andalas University, Padang City, Indonesia.

resins [5] can be engineered for specific binding, although they are not biodegradable and are associated with a larger environmental footprint. Zeolites [6] with their crystalline microporous lattices and cation-exchange properties have also been explored, but their efficiency in retaining glyphosate from aqueous solutions is often modest because of steric and polarity mismatches. MOFs [7], on the other hand, provide highly tunable pore systems and functional groups; however, their high cost of synthesis and poor stability in humid environments restrict their application at scale.

One promising approach is the utilization of agricultural and industrial residues such as palm oil mill waste, which is abundantly available in oil palm-producing countries. Indonesia is the world's largest producer of palm oil, recording a production of 43.5 million tons in 2020, far exceeding Malaysia's output of 19.9 million tons [8]. According to the Directorate General of Plantations, Ministry of Agriculture of Indonesia, the cultivated area of oil palm expanded from 14.66 million hectares in 2021 to 15.38 million hectares in 2022, and is projected to reach around 16.83 million hectares by 2023 [9]. The rapid expansion of palm oil plantations consequently leads to a substantial increase in palm oil mill residues, particularly oil palm empty fruit bunch (OPEFB) and wet decanter solid (WDS). If not managed properly, these waste materials pose significant environmental concerns. Elements present in WDS include calcium (Ca), phosphorus (P), nitrogen (N), potassium (K), and magnesium (Mg).

The disposal of WDS has been a serious concern for palm oil mills, as it is mostly dumped openly around factory sites and nearby landfills, causing pollution hazards and water contamination [10]. Similarly, OPEFB represents the most significant fraction of solid waste generated during fresh fruit bunch (FFB) processing and is emerging as a major production challenge in the palm oil industry [11]. Conventional uses of OPEFB include secondary products such as ash, biochar, and compost [12], and it is also commonly applied directly as mulch and organic fertilizer in soil [13]. Beyond their agronomic value, it is particularly interesting to evaluate their capacity to immobilize agrochemical pollutants, such as glyphosate, thereby linking waste valorization with environmental remediation. This dual function highlights the potential role of palm oil mill derivatives not only in supporting soil health, but also in mitigating herbicide contamination. Through thermochemical [14] and biochemical [15] conversion processes, such residues can be valorised into functional adsorbents, including biochar and humic substances. These materials exhibit large surface areas and abundant functional groups [16], providing considerable potential for the adsorption and immobilization of organic contaminants in soil and water systems.

Biochar, produced through the pyrolysis of biomass under limited oxygen conditions, possesses a high specific surface area, porous structure, and abundant functional groups (e.g. $-OH$, $-COOH$) that are capable of adsorbing various organic compounds [17], including pesticides like glyphosate. Meanwhile, sludge from WDS is rich in humic substances and dissolved organic matter, which also contributes to the immobilization of herbicides in soil through chemical interactions and surface binding [4]. Recent studies have emphasized the effectiveness of such materials in adsorbing agrochemicals [3–6], but further exploration is needed to understand their adsorption behaviour under varying environmental conditions, including concentrations. In this framework, Isothermal modelling emerges as a key analytical method for investigating the interactions between glyphosate molecules and the adsorbent surface. The application of models such as Henry, Freundlich, and Langmuir isotherms [18] offers valuable insights into the adsorption mechanisms and capacities, thereby enhancing our understanding of the performance and practical viability of these materials in environmental applications. Although biochar and humic substances have been widely studied [15,19–22], the combined utilization of biochar from OPEFB and humic substances from WDS as adsorbents for glyphosate has not been extensively reported. This specific combination, derived from palm oil mill waste, was emphasized as the novelty of this study. Accordingly, this study aims to evaluate the adsorption characteristics of glyphosate herbicide in solution using biochar and humic substances derived from the conversion of palm oil mill waste, and to model their adsorption behavior through Henry, Freundlich, and Langmuir isotherms. The findings are expected to contribute not only to the management of herbicide contamination but also to the promotion of sustainable waste utilization in plantation systems.

Materials and Methods

Conversion of palm oil mill waste

The study was carried out from September 2024 to February 2025 at the Chemistry and Soil Fertility Laboratory of the Soil Science and Land Resources Department, Faculty of Agriculture, and the Central Laboratory of Universitas Andalas. The primary raw material for biochar was freshly discarded oil palm empty

fruit bunch (OPEFB) waste, and humic substances were derived from wet decanter solid (WDS) collected from palm oil plantation in Dharmasraya, West Sumatra. The OPEFB was prepared following established methodologies [23], involving cleaning with running water, oven drying at 70 °C for 48 hours to dry and weighed for the production process with temperature of 200 °C for 30 minutes. To ensure consistency and standardization, each biochar production batch was prepared from 50 g of dry OPEFB waste, replicated three times. Pyrolysis was performed using an LMF-10D furnace, chosen for its precise temperature control and anaerobic conditions, which are vital for quality biochar. Humic substances were prepared from palm oil mill sludge obtained from WDS was oven-dried at 70 °C for 48 hours. The dried sludge was ground and sieved through a 2 mm mesh. A total of 5 g of the sieved sludge was weighed and mixed with 25 mL of 1 M technical-grade sodium hydroxide (NaOH) [24]. The mixture was shaken for 24 hours and then centrifuged at 4000 rpm for 15 minutes to separate the solid and liquid phases. The resulting filtrate was filtered using Whatman No. 41 filter paper. The supernatant was oven-dried at 70 °C for 24 hours. Biochar and humic substance then underwent morphological and characteristic laboratory analyses.

Following the preparation, the surface morphology of biochar (B-OPEFB) and humic substances (HS-WDS) was observed using a Scanning Electron Microscope (SEM, Carl Zeiss EVO 10) equipped with an Energy-Dispersive X-ray spectroscopy (EDX) detector. SEM provided high-resolution images of the surface structure, including pore distribution and texture. EDX was employed to determine the elemental composition of the samples, expressed as percentage by weight (%wt) of detected elements. The analysis covers the main elements of carbon, oxygen, silicon, potassium, magnesium, and calcium. The carbon content reported in this study was obtained directly from the EDX spectra, while the percentage of minerals was calculated automatically by the EDX software based on the relative intensity of characteristic X-ray peaks. The functional groups of B-OPEFB and HS-WDS were identified using Fourier Transform Infrared Spectroscopy (FTIR, Shimadzu FTIR Tracer-100). The spectra were recorded in the range of 4000–400 cm^{-1} with a resolution of 4 cm^{-1} . Samples were prepared in powder form and analyzed using the Attenuated Total Reflectance (ATR) technique. The FTIR spectra were used to detect characteristic absorption bands corresponding to hydroxyl (–OH), carboxyl (–COOH), carbonyl (C=O), C–H, and phosphate (P–O) groups, which are relevant to the adsorption interaction with glyphosate.

Determination of glyphosate herbicide concentration

The glyphosate herbicide used in this study was a commercial formulation, Supremo 486 SL, containing 356 g L^{-1} of glyphosate as the active ingredient. Its application rate was based on recommended field rates for oil palm plantations, proportionally converted to suit the scale of this laboratory study. To prepare the standard solutions, the herbicide was diluted with deionized water to obtain three concentrations of glyphosate application: 2.225, 6.675, dan 20.025 mg L^{-1} respectively. These concentrations were selected to simulate low, medium, and high application rates commonly used in oil palm plantations. Standard solutions were used in the batch equilibrium experiments to determine the adsorption behaviour of glyphosate in amended soils.

Isothermal adsorption experiment by batch equilibrium method

The isothermal adsorption of glyphosate in amended soil was evaluated using the batch equilibrium method. A total of 0.5 g of air-dried incubated soil (sieved to <2 mm) was weighed into a 100 mL Erlenmeyer flask. Each sample was treated with 20 mL of glyphosate solution at one of the three concentrations: 2.225, 6.675, and 20.025 mg L^{-1} . The soil samples were amended with five types of, including biochar from oil palm empty fruit bunches (B-OPEFB), humic substances extracted from wet decanter solid (HS-WDS), and their mixtures in three ratios: 75% B-OPEFB + 25% HS-WDS, 50% B-OPEFB + 50% HS-WDS, and 25% B-OPEFB + 75% HS-WDS. The experiment was arranged in a Completely Randomized Design (CRD) with three replications for each treatment. Each adsorbent mixture was thoroughly homogenized with the soil prior to glyphosate application.

After adding the glyphosate solution, the mixtures were shaken at 300 rpm for 24 hours at 25°C to reach adsorption equilibrium. Following incubation, the suspensions were centrifuged at 4000 rpm for 30 minutes to separate the liquid and solid phases. The resulting supernatants were filtered using Whatman No. 41 filter paper and subsequently analysed for residual glyphosate concentration using High-Performance Liquid Chromatography (HPLC, Shimadzu LC-20A). The HPLC system was equipped with a C18 reversed-phase column (4.6 × 250 mm, 5 μm) operated at 25 °C, with an injection volume of 20 μL and a detection wavelength of 200 nm. The mobile phase consisted of distilled water and methanol (80:20, v/v) at a flow rate of 1.0 mL min^{-1} . Calibration was performed using external glyphosate standards at concentrations of 2.225, 6.675, and

20.025 mg L⁻¹. This method was used to quantify the amount of glyphosate remaining in solution after equilibrium and to evaluate the adsorption behavior of the different adsorbent formulations under controlled laboratory conditions.

Adsorption Isotherm Model

To understand the mechanism and capacity of glyphosate adsorption onto biochar and humic substance-based materials, the experimental data were fitted to three common isotherm models: Henry, Freundlich, and Langmuir (Table 1). Each model provides different assumptions about the nature of adsorption surfaces and interactions, offering insights into the adsorption behavior of the tested materials.

Table 1. Linear and nonlinear isotherm equations for glyphosate adsorption onto solid surface. The table presents mathematical forms and plots of Henry, Freundlich, and Langmuir models, which have been used to analyze the adsorption capacity (Q_e) and equilibrium concentration (C_e). These equations were utilized in this study to determine the best fitting isotherm model for glyphosate adsorption.

Isotherm Model	Non-linear*	Linear	Plot	References
Henry	$Q_e = K_H \cdot C_e$	$Q_e = K_H \cdot C_e$	Q_e vs C_e	[25]
Freundlich	$Q_e = K_F \cdot C_e^{1/n}$	$\text{Log}(Q_e) = \text{Log}K_F + \frac{1}{n} \text{Log}C_e$	$\text{Log } Q_e$ vs $\text{Log } C_e$	[26]
Langmuir	$Q_e = \frac{Q_m \cdot K_L \cdot C_e}{1 + K_L \cdot C_e}$	$\frac{1}{Q_e} = \frac{1}{Q_m} + \frac{1}{Q_m K_L} \cdot \frac{1}{C_e}$	$\frac{1}{Q_e}$ vs $\frac{1}{C_e}$	[27]

* Q_e : adsorption capacity at equilibrium (mg g⁻¹), C_e : equilibrium concentration (mg L⁻¹), K_H : Henry constant (L g⁻¹), K_F : Freundlich constant ((mg g⁻¹)(L mg⁻¹)^{1/n}), K_L : Langmuir constant (L mg⁻¹).

Henry's isotherm model represents the most basic approach to understanding adsorption, asserting a linear relationship between the surface adsorbate quantity and the partial pressure of the adsorptive gas. This model effectively characterizes adsorbate behavior at low concentrations, assuming that each adsorbate molecule is spatially separated from its immediate surroundings [28]. The Freundlich adsorption isotherm model serves to describe a reversible and non-ideal adsorption phenomenon. Unlike models limited to single-layer coverage, the Freundlich model allows for the possibility of multilayer adsorption. A crucial feature of this isotherm is that it does not presuppose a uniform distribution of adsorption heat or affinities across a heterogeneous surface. Instead, the mathematical expression of the Freundlich isotherm model inherently accounts for surface heterogeneity, providing a definition for the exponential distribution of active sites and their respective energies [29]. The Langmuir isotherm is an empirical model positing that adsorption occurs as a single molecular layer (monolayer) on homogeneous, localized sites. Key assumptions include no steric hindrance or lateral interactions between adsorbed molecules, even on adjacent sites. This model further presumes that each molecule possesses uniform sorption activation energy and constant enthalpies, with all sites exhibiting equal affinity for the adsorbate and no adsorbate movement across the surface [30].

Experimental data modelling

Experimental data obtained from batch equilibrium studies were used to evaluate the adsorption behaviour of glyphosate onto converted palm oil mill waste materials. The amount of glyphosate adsorbed at equilibrium (Q_e) was calculated by subtracting the equilibrium concentration (C_e) from the initial concentration (C_0) using the following mass balance equation (Equations 1 and 2) [31].

$$Q_e = \left(\frac{C_0 - C_e}{m} \right) \times V \quad (1)$$

$$\%R = \left(\frac{C_0 - C_e}{C_0} \right) \times 100 \quad (2)$$

where Q_e is the adsorption capacity (mg g⁻¹), C_0 is the initial concentration (mg L⁻¹), C_e is the equilibrium concentration (mg L⁻¹), V is the volume of the glyphosate solution (L), and m is the amount of the of adsorbent used (g).

The adsorption data were then fitted to three isotherm models to describe the adsorption mechanism and to estimate the adsorption parameters. Non-linear and linear forms of each isotherm model were applied to the data. Linear regression analysis was conducted using Microsoft Excel and JMP software to determine the model constants and to evaluate the fit through the coefficient of determination (R^2). The best-fitting model was selected based on R^2 values and the consistency of estimated parameters with experimental trends. This modelling approach provided insights into the adsorption mechanisms and enabled comparison among

different adsorbent formulations, thereby supporting the selection of the most effective material for glyphosate removal.

Results

Morphological characteristics and elemental composition

The morphological characteristics and elemental composition of the palm oil mill waste-derived adsorbents are shown in Figure 1. The morphology of the two amendments differed in terms of color. Biochar derived from oil palm empty fruit bunch (B-OPEFB) appeared black, resembling charcoal typically produced from biomass or organic wastes. This coloration is associated with the high carbon content that underwent carbonization during pyrolysis, where most volatile and organic components were removed, leaving a stable carbon matrix behind.

The morphology, size, and shape of submicron particles can be characterized using SEM [32]. Based on SEM-EDX analysis of each amendment at 4000× magnification (scale 4 µm), B-OPEFB exhibited a porous structure with numerous elongated cavities and open channels, indicating the presence of well-developed pores and a heterogeneous surface. The surface appeared irregular and rough, consistent with the carbonized nature of biochar, significantly affect the resulting biochar morphology. The carbon content of B-OPEFB (83.17%) was the highest among the two tested amendments (B-OPEFB > HA-WDS, 25.99%), reflecting its nature as a carbon-rich material. Pyrolysis selectively retains carbon in the form of biochar while removing most volatile and non-carbon elements from biomass [21]. This process decomposes the majority of organic constituents such as hydrogen, oxygen, and nitrogen, while stabilizing carbon within the biochar matrix. Consequently, biochar exhibits a high carbon content and strong chemical stability, making it resistant to degradation [33]. In this study, oxygen in B-OPEFB accounted for 15.78%, whereas K, Mg, and Ca were present at 0.66%, 0.21%, and 0.19%, respectively.

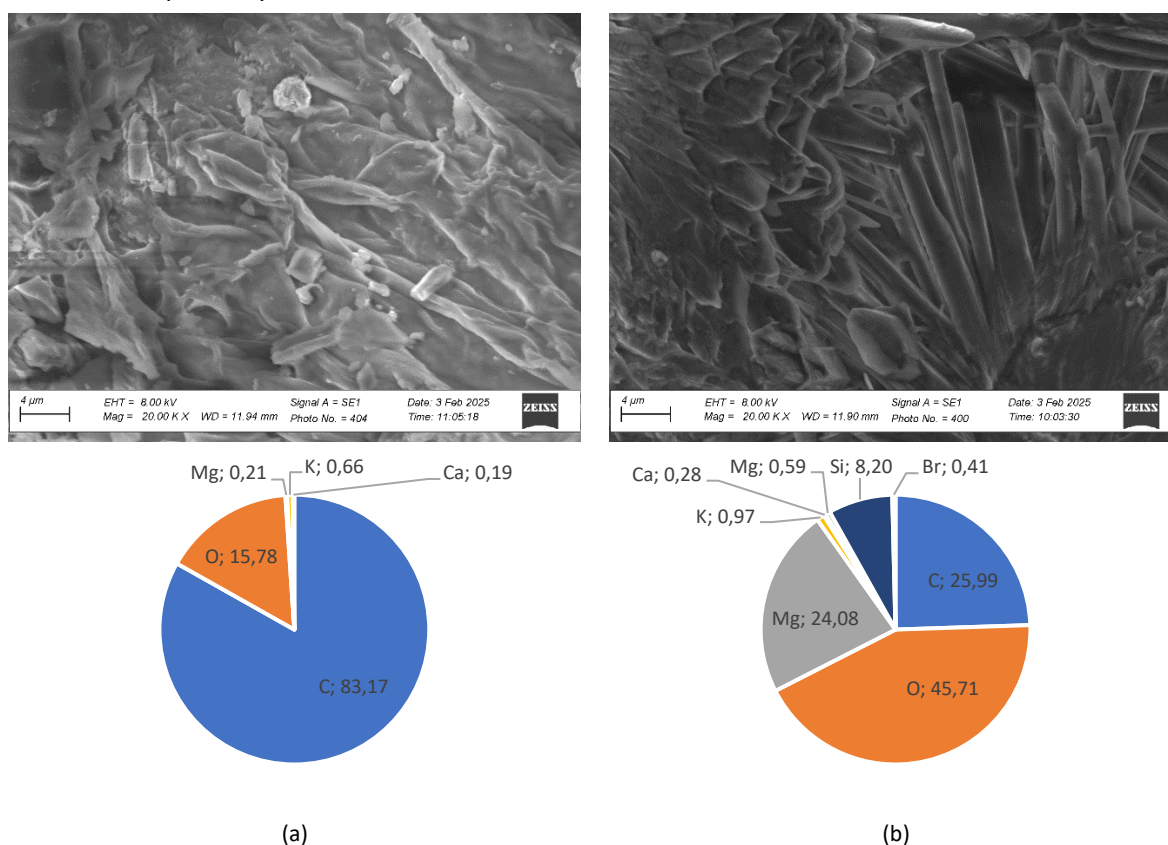


Figure 1. SEM-EDX images and elemental compositions of biochar produced from (a) oil-palm empty-fruit bunch and (b) humic substances derived from wet decanter solids.

The micrographs revealed differences in surface textures: the B-OPEFB was porous and disordered, while HS-WDS was denser and appeared smooth. The EDX pie charts confirmed that carbon and oxygen predominated

with the potential for carbon enrichment in the biochar and oxygen-rich functional groups of the humic substances. The humic substances extracted from wet decanter solids (HS-WDS) exhibited a compact and layered morphology with relatively smooth textures, as observed in the SEM images. The surface appeared dense with fewer open pores than that of B-OPEFB, indicating a more consolidated structure. The EDX analysis confirmed that oxygen (45.71%) was the dominant element, followed by carbon (25.99%), silicon (8.20%), potassium (0.97%), magnesium (0.59%), calcium (0.28%), and trace bromine (0.41%). The relatively high oxygen content reflects the abundance of oxygen-containing functional groups (OH, –COOH), which are typically enriched during alkaline extraction. NaOH activation has been reported to enhance the solubility of organic fractions by breaking down high molecular weight structures, releasing aromatic fragments, and increasing the oxygen content while reducing carbon [34]. In addition, Na incorporation during alkaline treatment promoted the formation of new hydroxyl and carboxyl groups on the material surface [35]. These structural and compositional changes explain the compact morphology of HS-WDS and its potential for strong chemical interactions, making it particularly effective for adsorption processes involving polar organic molecules, such as glyphosate.

Adsorption characteristics

The adsorption characteristics of glyphosate on the prepared adsorbents were evaluated to determine its effectiveness and interaction mechanisms, as summarized in Table 2. The glyphosate concentration influences the adsorption process because it is related to the ratio between the number of active sites of the amendment formulations and the glyphosate molecules available for interaction. In general, increasing the glyphosate concentration can enhance the adsorption capacity (Q_e) and the adsorption coefficient (K_a). However, the removal efficiency (R) tended to decrease, which may be attributed to the progressive saturation of adsorption sites at higher solute concentrations. In addition, a slight increase in solution pH was observed after adsorption (from an initial pH of 4.4–4.6 to 4.6–5.2), suggesting that proton exchange and the interaction of glyphosate functional groups with the adsorbent surface contributed to the overall adsorption process. The adsorption capacity (Q_e) represents the specific amount of adsorbate retained on the surface of the adsorbent [36].

Table 2. Equilibrium adsorption characteristics of glyphosate using biomaterials produced from palm oil mill waste. Overview of the adsorption mechanism of various formulations containing different amounts of biochar and humic substances. The adsorption capacity and removal efficiency were highest in the 25 % biochar + 75 % humic-substance formulation, which also promoted a slight increase in pH.

Bioconversion of Palm Oil Mill Waste	C_0^* mg L ⁻¹	C_e^*	pH of Glyphosate Solution Unit	Q_e^* mg g ⁻¹	R^* %	K_d^* L g ⁻¹	pH After Adsorption Unit
B-OPEFB*	2.225	2.34	4.4	88.91	99.89	38.00	4.6
	6.675	6.51	4.5	266.74	99.90	40.95	4.7
	20.025	7.23	4.6	800.71	99.96	110.76	4.8
HS-WDS*	2.225	1,195.56	4.4	41.18	46.27	0.03	4.7
	6.675	1,405.30	4.5	210.79	78.95	0.15	4.8
	20.025	1,462.66	4.6	742.49	92.70	0.51	4.9
75% B-OPEFB + 25% HS-WDS	2.225	140.98	4.4	83.36	93.66	0.59	4.8
	6.675	160.11	4.5	260.60	97.60	1.63	4.9
	20.025	162.32	4.6	794.51	99.19	4.89	5.0
50% B-OPEFB + 50% HS-WDS	2.225	177.82	4.4	81.89	92.01	0.46	4.9
	6.675	429.14	4.5	249.83	93.57	0.58	5.0
	20.025	552.76	4.6	778.89	97.24	1.41	5.1
25% B-OPEFB + 75% HS-WDS	2.225	928.70	4.4	51.85	58.26	0.06	5.0
	6.675	1,208.16	4.5	218.67	81.90	0.18	5.1
	20.025	1,261.86	4.6	750.53	93.7	0.59	5.2

*B-OPEFB: biochar-oil palm empty fruit bunch, HS-WDS: humic substance-wet decanter solid; C_0 : the initial concentration of the adsorbate, C_e : equilibrium concentration, Q_e : adsorption capacity, R : removal efficiency, K_d : Coefficient adsorption.

Table 2 presents the data on the equilibrium adsorption characteristics of glyphosate herbicide using converted palm oil mill waste in solution. Five types of adsorbents are compared: B-OPEFB, HS-WDS, and three mixtures of these in varying ratios (75:25, 50:50, 25:75). Among all treatments, B-OPEFB exhibited the highest adsorption capacity (Q_e) and adsorption coefficient (K_a), particularly at the highest initial concentration ($C_0 = 20,025 \text{ mg L}^{-1}$). At this level, B-OPEFB achieved $Q_e = 800.71 \text{ mg g}^{-1}$, $K_a = 110.76 \text{ L g}^{-1}$, and a nearly complete removal efficiency (R) of 99.96%. The adsorption coefficient (K_d) reflects the ability of a molecule to be retained on the adsorbent surface [18]. This superior performance is consistent with the highly porous and carbon-rich structure of biochar, which provides abundant active sites for physical adsorption. Adsorbents with porous structures can increase the surface area available for adsorption. This structure creates more contact points between the adsorbent and the energy to be absorbed [21].

As the glyphosate concentration in the solution increased, more molecules became available for interaction, thereby occupying a greater number of adsorption sites on the amendment surface. This process, in turn, enhances the adsorption coefficient because of the combined physical and chemical interactions between glyphosate and the adsorbent surface. In contrast, HS-WDS showed the less adsorption performance, with Q_e values ranging from 41.18 to 742.49 mg g^{-1} and K_a values not exceeding 0.51 L g^{-1} . The removal efficiency was also lower (46.27–92.70%), which can be attributed to its compact morphology and relatively fewer physical adsorption sites. However, its high oxygen content may contribute to chemical interactions, particularly through hydrogen bonding and electrostatic attraction, although it is less efficient than biochar.

The combination treatment exhibited synergistic effects. The 75% B-OPEFB + 25% HS-WDS formulation recorded a high adsorption capacity ($Q_e = 794.51 \text{ mg g}^{-1}$) and removal efficiency ($R = 99.19\%$) at $C_0 = 20,025 \text{ mg L}^{-1}$, with a K_a value of 4.89 L g^{-1} . Similarly, the 50:50 mixture reached $Q_e = 778.89 \text{ mg g}^{-1}$, $R = 97.24\%$, and $K_a = 1.41 \text{ L g}^{-1}$ under the same conditions. The %R value is used to evaluate the effectiveness of an adsorbent in removing or reducing an adsorbate from a solution or medium [37]. Although lower than pure biochar in terms of Q_e and K_a , these mixtures still performed significantly better than the HS-WDS alone, highlighting the complementary roles of biochar and humic substances. Biochar contributes to physical sorption via its porous carbon matrix, whereas HS-WDS enhances the chemical interactions through oxygen-containing functional groups. The 25% B-OPEFB + 75% HS-WDS mixture, while containing a higher proportion of humic material, also achieved relatively high adsorption performance ($Q_e = 750.53 \text{ mg g}^{-1}$, $R = 93.70\%$). This confirms that humic substances can play a supporting role, especially in enhancing surface reactivity, whereas biochar remains the dominant contributor to glyphosate immobilization.

The mixture treatments demonstrated synergistic effects, where the combination of B-OPEFB and HS-WDS resulted in a higher adsorption performance compared to HS-WDS alone. This improvement can be explained by the complementary mechanisms of the two materials. B-OPEFB has a porous carbon-rich structure with a large surface area, favoring physical adsorption through pore entrapment and hydrophobic interactions [21]. Meanwhile, HS-WDS provides abundant oxygen-containing functional groups ($-\text{OH}$, $-\text{COOH}$), which facilitate chemical interactions such as hydrogen bonding, ligand exchange, and electrostatic attraction [34]. The integration of these mechanisms enhances glyphosate immobilization by combining the high surface area of biochar with the chemical reactivity of humic substances. Similar synergistic effects of biochar–humic mixtures have been reported in previous studies. Combining kaolinite with humic acid increases glyphosate adsorption due to improved surface heterogeneity and functional group diversity [4]. Similarly, biochar has been shown to improve the sorption of pesticides and heavy metals in soils by providing multiple binding sites and stabilizing the adsorbed molecules [19]. These findings support the observation in this study that biochar and humic mixtures, particularly at 75:25 and 50:50 ratios, provide a favourable balance between physical sorption capacity and chemical reactivity, leading to enhanced removal efficiency.

Surface characteristic

FTIR analysis provides information about the functional groups in different adsorbents, which might facilitate the sorption process. FTIR lies in the interaction between infrared radiation and the chemical bonds within molecules. Distinctive absorption bands were attributed to various functional groups (e.g., C-H, O-H, C=O, C-C) possesses by its own characteristic vibrational frequencies. Specifically, O=C=O stretching modes were observed at 2348 and 1030 cm^{-1} [38]. Concurrently, C-O stretching vibrations were identified within the wavenumber range of 1022 to 1123 cm^{-1} [39]. O-H wavenumbers ranging from 3400 to 3600 cm^{-1} [40]. The FTIR spectrum in Figure 2 shows changes in the characteristics of the functional groups on the surface of the material before and after glyphosate adsorption. In B-OPEFB, the hydroxyl group ($-\text{OH}$) which originally appeared at 3464.15 cm^{-1} shifted to 3402.49 cm^{-1} after adsorption, indicating the formation of hydrogen bonds between glyphosate and the biochar surface. The absorption band at 1608.63 cm^{-1} (N-H and C=C

bending) shifted to 1615.41 cm^{-1} , the band at 1263.37 cm^{-1} associated with the C–O group changed slightly after adsorption, indicating phosphonate interactions.

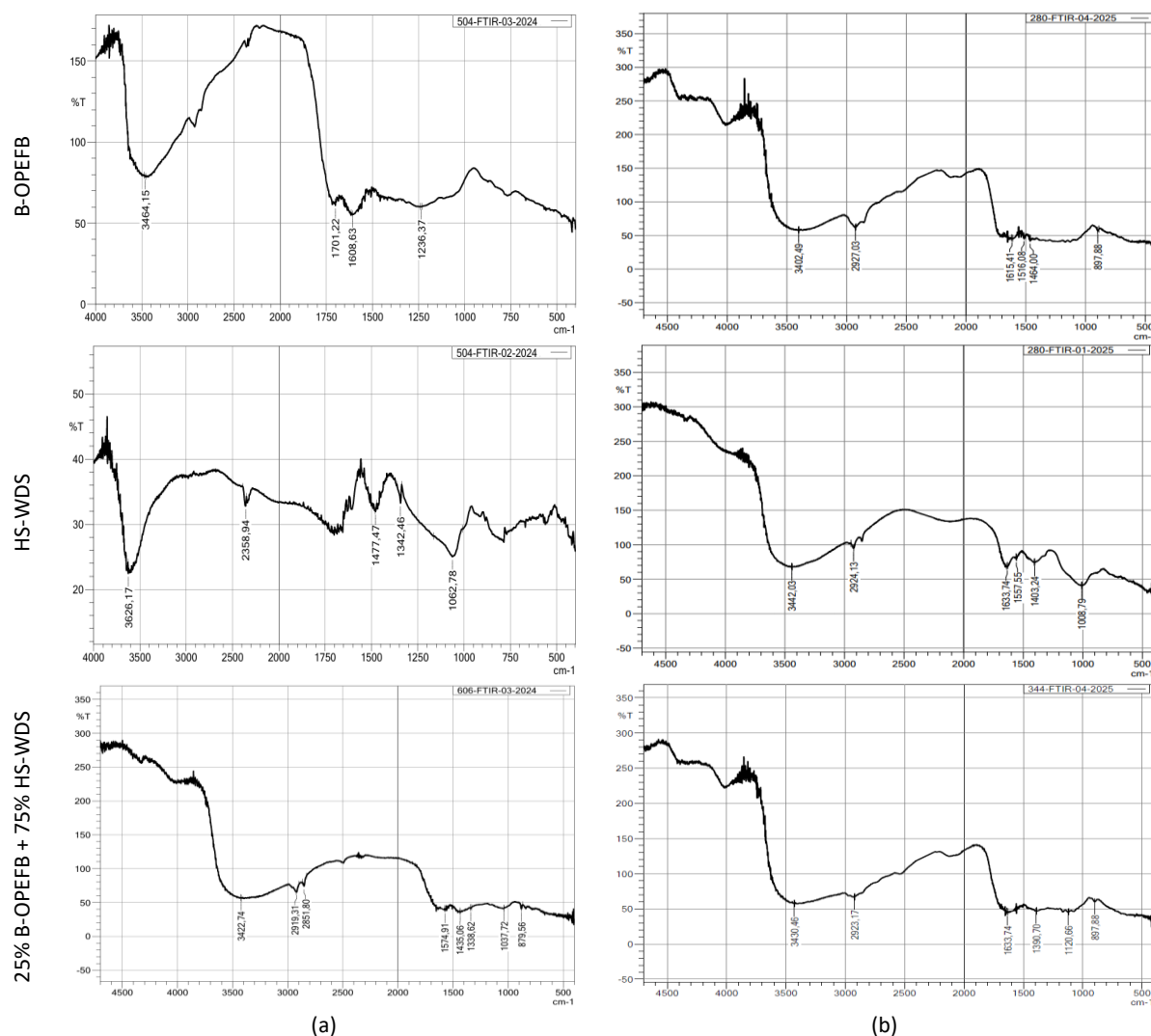


Figure 2. FTIR spectra using biochar and humic substances obtained from palm oil mill waste (a) before glyphosate adsorption and (b) after glyphosate adsorption.

The spectra show significant changes in the peaks around –OH, C=O, and P–O functional groups, indicating their contribution to glyphosate binding on the adsorbent surface. For HS-WDS, the O–H absorption band at 3626.17 cm^{-1} shifted to 3442.03 cm^{-1} after adsorption. The O=C=O band, which was originally seen at 2358.94 cm^{-1} [41] disappeared, indicating its involvement in adsorption. In addition, the C–H bending bands at 1477.47 cm^{-1} and 1342.46 cm^{-1} shifted or decreased to 1633.74 and 1403.24 cm^{-1} , as well as the C–O/P–O band from 1062.78 cm^{-1} to 1008.79 cm^{-1} , indicating the presence of a bond formed with the phosphonate group of glyphosates. The emergence of a new band at 2924 cm^{-1} after adsorption on HS-WDS indicates the presence of asymmetric C–H stretching vibrations [42], which are likely to originate from the aliphatic group in the glyphosate structure. This band was not detected before adsorption, indicating that glyphosate molecules successfully interacted with the adsorbent surface and caused changes in the vibrational spectrum. The FTIR spectra of the mixture of 25% B-OPEFB and 75% HS-WDS before and after glyphosate adsorption also showed a shift in the main absorption bands. This shift indicated that the functional groups present on the surface of the adsorbent played a role in the interaction and adsorption of glyphosate molecules.

Analysis of the data demonstrated clear evidence of interaction and adsorption. This is supported by the fact that some functional groups vanished entirely after the adsorption process, whereas others showed changes in their characteristic adsorption frequencies. The emergence of new functional groups further confirms that the process involves the active participation of these functional groups, consistent with findings from other sources [43]. These results indicate that the various oxygen-containing functional groups on the surface of

both humic substances and biochar are crucial for their interaction with glyphosate. Specifically, the hydrophilicity of hydroxyl (-OH) groups and the strong acidity of carboxyl (-COOH) groups can directly or indirectly influence their binding performance with aqueous contaminants, such as glyphosate, and the stability of the resulting adsorbed complexes [44]. Certain functional groups, such as -OH, -C=O, and -C-OH, are vital for providing active adsorption sites and electroactive sites. These sites, which can act as electron donors (e.g., hydroxyl groups) and acceptors (e.g. ketones or quinones), are generally beneficial for facilitating the efficient binding and removal of glyphosate [16]. The emergence of various functional groups on the surface of biochar and humic substances plays a pivotal role in adsorption mechanisms. This surface functionality can directly or indirectly influence the ability of both materials to bind glyphosate, thereby enhancing the adsorption efficiency and capacity of herbicides.

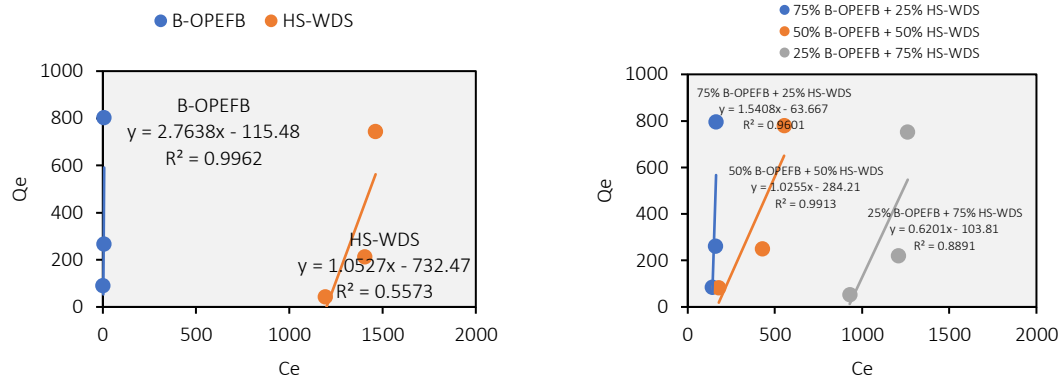
Isotherm of adsorption

Adsorption isotherm models can be used to describe the distribution of adsorbate molecules on an adsorbent when the adsorption process reaches equilibrium. The Freundlich and Langmuir isothermal models were applied to evaluate the adsorption of glyphosate and determine the most appropriate and optimal adsorption process, considering the high R^2 values [45]. The adsorption of glyphosate using the ameliorant formulations showed that the linear R^2 values of both the models differed. However, they exhibited a similar trend with respect to the combination and percentage composition of ameliorant formulations.

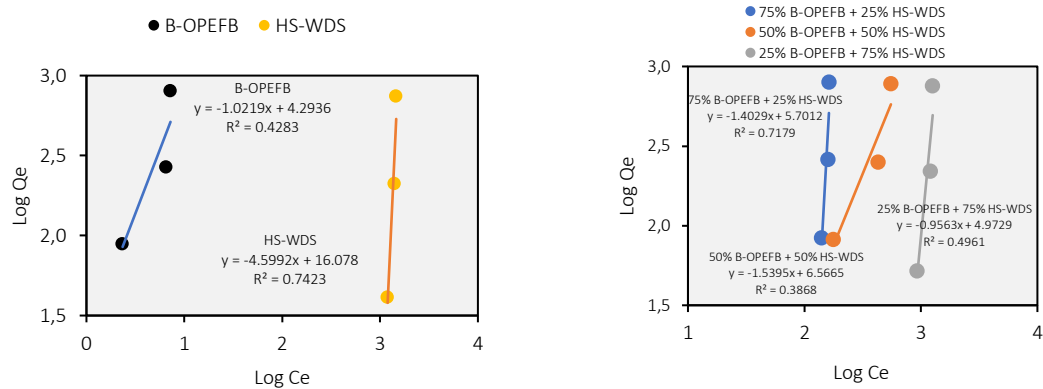
Isotherm modeling results demonstrate varying glyphosate adsorption mechanisms depending on the adsorbent type. B-OPEFB (biochar) best fit the Henry model ($R^2 = 0.9962$), indicating linear interactions at low concentrations, consistent with its highly porous carbon structure that provides abundant physical sorption sites [40]. Conversely, the pure HS-WDS (humic substances) showed a very strong correlation with the Langmuir model ($R^2 = 0.9808$), suggesting dominant monolayer adsorption on homogeneous sites, although it also presented a moderate fit with the Freundlich model ($R^2 = 0.7423$), implying surface heterogeneity. Notably, the Langmuir model generally provided the best overall fit for most biochar and humic substance combinations, particularly for the 25% B-OPEFB + 75% HS-WDS ($R^2 = 0.9785$) and 50% B-OPEFB + 50% HS-WDS ($R^2 = 0.9689$) mixtures. This indicates that the predominant adsorption mechanism in these mixtures is monolayer formation on a relatively homogeneous surface, likely due to the synergistic effect of the porous biochar structure, which enhances the surface area and humic substances supplying reactive functional groups.

The results of glyphosate adsorption isotherm modelling on B-OPEFB, HS-WDS, and their combinations (Table 3) provided in-depth insight into the interaction mechanism between glyphosate and the tested adsorbents. The selection of the best isotherm model was based on the coefficient of determination (R^2) value closest to 1, indicating agreement between the experimental data and the model assumptions. The glyphosate adsorption on pure B-OPEFB showed a very good fit with the Henry model ($R^2 = 0.9962$), indicating a strong linear interaction at low glyphosate concentrations. This is consistent with the assumption of the Henry model that adsorption sites are abundant and not yet saturated, which is typical of the early stage of adsorption. Nevertheless, B-OPEFB also showed a good fit with the Langmuir model ($R^2 = 0.9169$, Figure 3c), with a maximum monolayer adsorption capacity (Q_m) of 333.33 mg g^{-1} and a separation factor (R_L) of 0.0002, indicating highly favourable and nearly irreversible adsorption. However, the Freundlich model did not fit B-OPEFB ($R^2 = 0.4283$), implying that the biochar surface was relatively homogeneous and did not show significant heterogeneity in the distribution of adsorption sites. Functional groups such as -OH and C=C on B-OPEFB (FTIR Figure 2a) likely played a role in providing these homogeneous adsorption sites.

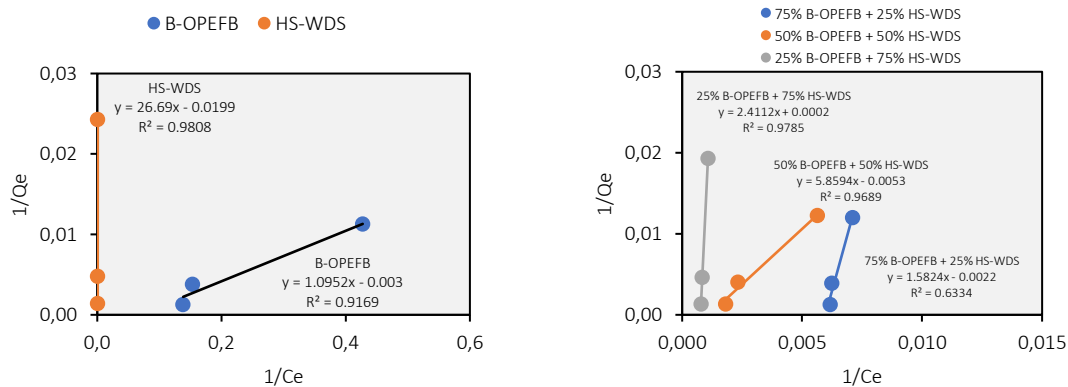
HS-WDS showed interesting adsorption behaviour. Despite having $n=0.22$ in the Freundlich model, which theoretically [46] indicates a highly heterogeneous surface and moderate fit ($R^2 = 0.7423$, Figure 3b), HS-WDS showed a much better fit with the Langmuir model ($R^2 = 0.9808$, Figure 3c). The very low R_L value (0.0002) confirmed that glyphosate adsorption on HS-WDS had a significantly stronger fit. The Q_m capacity of HS-WDS was 50.25 mg g^{-1} , which was lower than that of B-OPEFB, indicating that the monolayer adsorption sites on HS-WDS operated efficiently. The dominance of the Langmuir fit ($R^2 = 0.9808$) indicated that, despite the possible heterogeneity, glyphosate tended to adsorb as a monolayer on specific and homogeneous sites on the HS-WDS surface. The abundance of functional groups such as carboxyl (-COOH) and hydroxyl (-OH) in HS-WDS (FTIR Figure 2a), which are known to have a high affinity for glyphosate through hydrogen bonding and electrostatic interactions, may explain this efficient monolayer adsorption capacity.



(a)



(b)



(c)

Figure 3. Experimental glyphosate adsorption isotherm models using (a) Henry, (b) Freundlich, and (c) Langmuir models, utilizing conversion from palm oil mill effluent.

The graphs show the various adsorption behaviors observed, with the Langmuir model being the best fit, indicating that monolayer adsorption occurs on a relatively uniform surface. Overall, the Langmuir model provided the best fit for almost all adsorbent combinations (Figure 3c), confirming that the dominant adsorption mechanism was a monolayer on a relatively homogeneous surface for this mixture system. The most prominent fit was observed for the mixtures of 25% B-OPEFB + 75% HS-WDS ($R^2 = 0.9785$) and 50% B-OPEFB + 50% HS-WDS ($R^2 = 0.9689$). The mixture of 25% B-OPEFB and 75% HS-WDS showed an exceptionally high maximum monolayer adsorption capacity (Q_m) of 5000 mg g^{-1} . This capacity far exceeds the adsorption capacity of each pure component, even exceeding 75% B-OPEFB + 25% HS-WDS ($Q_m = 454.55 \text{ mg g}^{-1}$). This indicated a strong synergistic effect between biochar and humic substances at a certain proportion. The complementary interactions between the functional groups of B-OPEFB and HS-WDS, such as hydroxyl,

carboxyl, and aromatic groups (FTIR Figure 2a), most likely create more available adsorption sites or increase the affinity of existing sites, thus facilitating the formation of a denser and more stable glyphosate monolayer.

Table 3. Isothermal adsorption parameters obtained from the Freundlich and Langmuir models using biochar and humic substances produced from palm oil mill waste. The table displays adsorption constants and correlation coefficients (R^2) with linearized equations for the goodness of fit of each model. The higher the Langmuir correlation values, the more dominant is the monolayer adsorption mechanism.

Adsorbents	Isothermal			
	Freundlich			
	n	K_F (mg g^{-1}). (L mg^{-1}) ⁿ	1/n	Linear Equations
B-OPEFB	0.98	19,669.75	1.02	$y = -1.0219x + 4.2936$; $R^2 = 0.4283$
HS-WDS	0.22	1.19×10^{16}	4.55	$y = -4.5992x + 16.078$; $R^2 = 0.7423$
75% B-OPEFB + 25% HS-WDS	0.71	502,573.98	1.41	$y = -1.4029x + 5.7012$; $R^2 = 0.7179$
50% B-OPEFB + 50% HS-WDS	0.65	3,685,530.42	1.54	$y = -1.5395x + 6.5665$; $R^2 = 0.3868$
25% B-OPEFB + 75% HS-WDS	1.04	93,950.69	0.96	$y = -0.9563x + 4.9729$; $R^2 = 0.4961$
Adsorbents	Langmuir			
	Q_m (mg g^{-1})	K_L (L mg^{-1})	R_L	Linear Equations
B-OPEFB	333.33	0.0027	0.0002	$y = 1.0952x - 0.003$; $R^2 = 0.9169$
HS-WDS	50.25	0.0007	0.0002	$y = 26.69x - 0.0199$; $R^2 = 0.9808$
75% B-OPEFB + 25% HS-WDS	454.55	0.0014	0.0002	$y = 1.5824x - 0.0022$; $R^2 = 0.6334$
50% B-OPEFB + 50% HS-WDS	188.68	0.0009	0.0002	$y = 5.8594x - 0.0053$; $R^2 = 0.9689$
25% B-OPEFB + 75% HS-WDS	5,000	0.0001	0.0002	$y = 2.4112x + 0.0002$; $R^2 = 0.9785$

B-OPEFB: biochar-oil palm empty fruit bunch, HS-WDS: humic substance-wet decanter solid, Freundlich [$n = 1/b$; $K_F = 10^3$], Langmuir [$Q_m = 1/a$; $K_L = a/b$], $R_L = 1/[1 + (K_L \cdot C_0)]$.

Discussion

The adsorption of glyphosate herbicide utilising biochar and humic substances sourced from palm oil mill waste presents considerable promise for environmental remediation efforts. This study demonstrates that the combined application of these materials, particularly the formulation comprising 25% B-OPEFB and 75% HS-WDS, exhibits an outstanding adsorption capacity ($5,000 \text{ mg g}^{-1}$) and efficiency, as reflected by the strong conformity to the Langmuir isotherm model ($R^2 = 0.9785$). This finding suggests that the adsorption mechanism is predominantly governed by monolayer formation at the homogeneous binding sites on the adsorbent surface. Such a high adsorption performance is consistent with earlier research [19], which showed that both biochar and humic substances are rich in functional groups that facilitate interactions with organic pollutants via hydrogen bonding, electrostatic interactions, and surface complexation. However, differences in feedstock properties can explain the variations in adsorption performance. Coconut residues generally contain lower ash and mineral fractions, whereas oil palm empty fruit bunches (OPEFB) are richer in lignocellulosic components and produce higher ash content with abundant minerals such as K, Ca, and Mg, which enhance electrostatic interactions. In addition, OPEFB is generated in far greater quantities in palm oil-producing countries, making it a more sustainable and cost-effective raw material than coconut waste. These inherent characteristics contributed to the superior adsorption capacity observed for OPEFB-derived biochar and its combination with HS-WDS in the present study. Various factors, including pH, adsorbent dosage, initial glyphosate concentration, and contact time, influence glyphosate adsorption [47]. In addition, the morphological characteristics of the material observed by SEM-EDX in this study played a significant role.

The adsorption process can be described by different isotherm models, such as the Langmuir and Freundlich models, which provide insights into adsorption capacity and mechanisms. The Langmuir model is particularly useful for understanding monolayer adsorption, whereas the Freundlich model describes multilayer adsorption [30]. In this study, the dominance of the Langmuir model suggests that glyphosate adsorption occurs primarily on specific, homogeneous sites, a phenomenon also observed in studies involving kaolinite-humic acid composites [4]. The exceptionally high Q_m value (5000 mg g^{-1}) obtained for the 25% B-OPEFB + 75% HS-WDS mixture may reflect either synergistic effects or model overestimation at high concentrations. Differences in adsorption sites and porosity can be directly correlated with the Q_m values, as larger surface areas and pore volumes typically yield higher maximum adsorption capacities [48]. For comparison, the effective surface area of sub-bituminous coal can reach $\geq 100 \text{ m}^2 \text{ g}^{-1}$ [49], whereas biochar exhibits a wide range of surface areas ($5.4\text{--}328.6 \text{ m}^2 \text{ g}^{-1}$), depending on feedstock and pyrolysis conditions [50]. Therefore, while the observed Q_m trend indicates a strong synergistic adsorption potential, the absolute value should be interpreted cautiously considering that isotherm extrapolation at high concentrations may artificially inflate the estimated maximum capacity.

The synergistic interaction between the components of the 25% B-OPEFB and 75% HS-WDS mixture is responsible for the improved performance. Physical adsorption is enhanced by the very large surface area and very fine pore structure of biochar. Humic compounds, on the other hand, add oxygen-containing functional groups to the mixture, such as hydroxyl ($-\text{OH}$) and carboxyl ($-\text{COOH}$), which increase the chemical affinity for glyphosate and facilitate more efficient binding and retention [51]. Biochar with higher carbon content generally has a darker color. The final color is also influenced by the pyrolysis temperature; higher temperatures generally produce darker biochar due to better carbon stabilization. In addition, the type of biomass used can affect both color and structural stability [52]. Humic compounds extracted from wet decanted solids (HS-WDS) using NaOH, on the other hand, have a deeper dark brown to almost black color compared to conventional humic extracts. The breakdown and dissolution of organic components during alkaline extraction, which alters the chemical structure of organic materials, is likely the cause of this change.

The final dark color and chemical characteristics can be further influenced by additional variables including extraction temperature, time, and reagent concentration [53]. The darker color of HS-WDS indicates the presence of concentrated organic residues and oxygen-rich functional groups ($-\text{OH}$, $-\text{COOH}$), which corresponds to the high oxygen content found through EDX analysis. The physical characteristics of biochar, such as its color, porosity, and functional group distribution, are significantly influenced by variables other than temperature and biomass type, such as pyrolysis residence time, applied pressure, and oxygen availability [54]. The theory of cooperation is supported by FTIR analysis (Figure 2). Following adsorption, the peaks of important molecules such $-\text{OH}$ and $\text{C}=\text{O}$ shift, suggesting that they aid in glyphosate retention. These discoveries have important environmental implications. It prevents glyphosate pollution and assist in waste management by recycling palm oil mill waste. In palm oil plantations, where glyphosate is frequently used, a combination of 25% B-OPEFB and 75% HS-WDS absorbs glyphosate very well and can assist enhance soil quality. Furthermore, following adsorption, the pH of the solution slightly increased (from 4.6 to 5.2), which is great for agriculture since it prevents the soil from being overly acidic. Because it maintains the soil's ideal pH for microorganisms and nutrients, this pH range is perfect for plants [55].

Standardizing application techniques and comprehending long-term effects are still difficulties, despite the chemical interaction between biochar and humic substances showing promise for enhancing soil and environmental health. The effects of biochar and other materials on various soil types and environmental circumstances require more investigation. This use can lower hazards to aquatic habitats by lowering glyphosate runoff into nearby rivers on a landscape scale. By enhancing soil health and water quality at the watershed level, this amendment's implementation in oil palm plantation management is consistent with an integrated natural resource management approach. It is crucial to recognize a number of the study's limitations to guarantee the accuracy of these environmental advantages. The experiments were conducted under controlled laboratory and incubation conditions with a single soil type and herbicide, without kinetic or thermodynamic analyses, which restricts the generalization of the results. Moreover, the study focused on glyphosate residues after entering the soil, meaning that the implications for weed control effectiveness were not directly assessed. Future field validation across multiple soil types, other commonly used pesticides, and additional kinetic or thermodynamic studies are needed to provide a more comprehensive understanding of the adsorption behavior and its long-term implications in agricultural systems.

Conclusions

This study demonstrated that biochar produced from oil palm empty fruit bunches (B-OPEFB) and humic substances extracted from wet decanter solids (HS-WDS) effectively adsorbed glyphosate herbicides from aqueous solution. The adsorption process was best described by the Langmuir isotherm, particularly for the 25% B-OPEFB and 75% HS-WDS mixture, which showed an exceptionally high monolayer adsorption capacity (5,000 mg g⁻¹) with strong model fit ($R^2 = 0.9785$). FTIR analysis confirmed that hydroxyl (–OH), carboxyl (–COOH), and aromatic functional groups were actively involved in glyphosate binding through hydrogen bonding and electrostatic interactions. Beyond these laboratory findings, the broader significance of this study lies in demonstrating how agricultural residues can be transformed into effective remediation materials. Utilizing palm oil mill by-products as soil amendments provides a dual benefit: mitigating glyphosate contamination while promoting sustainable waste valorisation in oil palm landscapes. At the management level, incorporating such amendments into plantation practices can enhance soil health, reduce the leaching of agrochemicals into waterways, and support integrated watershed and natural resource management strategies. These outcomes are particularly relevant for policy frameworks aiming to reconcile intensive agricultural production with environmental sustainability.

Author Contributions

SA: Conceptualization, Methodology, Software, Investigation, Writing - Review & Editing; **YY:** Methodology, Review Supervision; **AM:** Conceptualization, Methodology, Writing - Review & Editing, Supervision; **HH:** Conceptualization, Methodology, Review, Supervision

Acknowledgments

The authors would like to acknowledge Andalas University for financial support under the Master's Thesis Research Scheme Batch I, according to Research Contract No. 160/UN16.19/PT.01.03/PTM/2025, Fiscal Year 2025.

AI Writing Statement

The authors did not use any artificial intelligence assisted technologies in the writing process.

Conflict of Interest

There are no conflicts to declare.

References

1. Gandhi, K.; Khan, S.; Patrikar, M.; Markad, A.; Kumar, N.; Choudhari, A.; Sagar, P.; Indurkar, S. Exposure Risk and Environmental Impacts of Glyphosate: Highlights on the Toxicity of Herbicide Co-Formulants. *Environ. Challenges* **2021**, *4*, 100149, doi:10.1016/j.envc.2021.100149.
2. Bueno de Mesquita, C.P.; Solon, A.J.; Barfield, A.; Mastrangelo, C.F.; Tubman, A.J.; Vincent, K.; Porazinska, D.L.; Hufft, R.A.; Shackelford, N.; Suding, K.N.; et al. Adverse Impacts of Roundup on Soil Bacteria, Soil Chemistry and Mycorrhizal Fungi during Restoration of a Colorado Grassland. *Appl. Soil Ecol.* **2023**, *185*, 104778, doi:10.1016/j.apsoil.2022.104778.
3. Menegazzo, F.; Snyders, R.; Bittencourt, C.; Carmen Bello Pinzon, M. Del; Ghedini, E.; Signoretto, M. From Waste to Adsorbent: Properties of CO₂-Activated Biochars from Pistachio Hulls and Walnut Shells for Advanced Water Remediation. *Bioresour. Technol.* **2026**, *439*, 133367, doi:10.1016/j.biortech.2025.133367.
4. Guo, F.; Zhou, M.; Xu, J.; Fein, J.B.; Yu, Q.; Wang, Y.; Huang, Q.; Rong, X. Glyphosate Adsorption onto Kaolinite and Kaolinite-Humic Acid Composites: Experimental and Molecular Dynamics Studies. *Chemosphere* **2021**, *263*, doi:10.1016/j.chemosphere.2020.127979.
5. Xu, M.; Zhang, L.; Yuan, L.; Ji, C.; Zhang, Y.; Kong, D.; Zhang, Y.; Lv, L.; Hua, M.; Zhang, W. Machine Learning-Assisted Adsorption Capacity Prediction of Ion Exchange or Chelate Resin for Heavy Metals in Aqueous Solutions: External Validation via Multi-Factor Experiments. *Sep. Purif. Technol.* **2025**, *368*, 133019, doi:10.1016/j.seppur.2025.133019.

6. Andrunik, M.; Skalny, M.; Gajewska, M.; Marzec, M.; Bajda, T. Comparison of Pesticide Adsorption Efficiencies of Zeolites and Zeolite-Carbon Composites and Their Regeneration Possibilities. *Heliyon* **2023**, *9*, e20572, doi:10.1016/j.heliyon.2023.e20572.
7. Yuan, L.; Chai, J.; Wang, S.; Li, T.; Yan, X.; Wang, J.; Yin, H. Biomimetic Laccase-Cu₂O@MOF for Synergetic Degradation and Colorimetric Detection of Phenolic Compounds in Wastewater. *Environ. Technol. Innov.* **2023**, *30*, 103085, doi:10.1016/j.eti.2023.103085.
8. Sidabutar, R.; Trisakti, B.; Irvan; Bani, O.; Nasution, J.A.; Khodijah, P.; Alexander, V.; Daimon, H.; Takriff, M.S. Treatment of Effluent from the Upflow Anaerobic Sludge Blanket-Hollow Centered Packed Bed Fermentor by Utilizing *Chlorella Vulgaris* in a Fed-Batch System. *Case Stud. Chem. Environ. Eng.* **2024**, *9*, 100756, doi:10.1016/j.cscee.2024.100756.
9. Oktaviani, M.; Kamaluddin, N.N.; Simarmata, T. A Enhancing the Composting Process and Quality of Oil Palm Empty Fruit Bunches (EFB) Using Indigenous Cellulolytic Microbes: A Review. *Int. J. Life Sci. Agric. Res.* **2024**, *3*, doi:10.55677/ijlsar/V03I4Y2024-09.
10. Ong, T.H.; Hamzah, M.H.; Che Man, H. Optimization of Palm Oil Extraction from Decanter Cake Using Soxhlet Extraction and Effects of Microwaves Pre-Treatment on Extraction Yield and Physicochemical Properties of Palm Oil. *Food Res.* **2021**, *5*, 25–32, doi:10.26656/fr.2017.5(S1).008.
11. Anyaoha, K.E.; Sakrabani, R.; Patchigolla, K.; Mouazen, A.M. Critical Evaluation of Oil Palm Fresh Fruit Bunch Solid Wastes as Soil Amendments: Prospects and Challenges. *Resour. Conserv. Recycl.* **2018**, *136*, 399–409, doi:10.1016/j.resconrec.2018.04.022.
12. Hariana; Prabowo; Hilmawan, E.; Milky Kuswa, F.; Darmawan, A.; Aziz, M. A Comprehensive Evaluation of Cofiring Biomass with Coal and Slagging-Fouling Tendency in Pulverized Coal-Fired Boilers. *Ain Shams Eng. J.* **2023**, *14*, 102001, doi:10.1016/j.asej.2022.102001.
13. Hau, L.J.; Shamsuddin, R.; May, A.K.A.; Saenong, A.; Lazim, A.M.; Narasimha, M.; Low, A. Mixed Composting of Palm Oil Empty Fruit Bunch (EFB) and Palm Oil Mill Effluent (POME) with Various Organics: An Analysis on Final Macronutrient Content and Physical Properties. *Waste and Biomass Valorization* **2020**, *11*, 5539–5548, doi:10.1007/s12649-020-00993-8.
14. Abel, R.S.E.; Loh, S.K.; Wahab, N.S.A.; Masek, O.; Musa, I.; Bachmann, R.T. Effect Of Operating Temperature On Physiochemical Properties Of Empty Fruit Bunch Cellulose-Derived Biochar. *J. Oil Palm Res.* **2021**, doi:10.21894/jopr.2021.0007.
15. Winarso, S.; Pandutama, M.H.; Purwanto, L.D. Effectivity of Humic Substance Extracted from Palm Oil Compost as Liquid Fertilizer and Heavy Metal Bioremediation. *Agric. Agric. Sci. Procedia* **2016**, *9*, 146–157, doi:10.1016/j.aaspro.2016.02.110.
16. Dai, L.; Lu, Q.; Zhou, H.; Shen, F.; Liu, Z.; Zhu, W.; Huang, H. Tuning Oxygenated Functional Groups on Biochar for Water Pollution Control: A Critical Review. *J. Hazard. Mater.* **2021**, *420*, doi:10.1016/j.jhazmat.2021.126547.
17. Fakhar, A.; Canatoy, R.C.; Jane, S.; Galgo, C.; Rafique, M.; Sarfraz, R. Advancements in Modified Biochar Production Techniques and Soil Application: A Critical Review. *Fuel* **2025**, *400*, 135745, doi:10.1016/j.fuel.2025.135745.
18. Raji, Z.; Karim, A.; Karam, A.; Khalloufi, S. Adsorption of Heavy Metals: Mechanisms, Kinetics, and Applications of Various Adsorbents in Wastewater Remediation—A Review. *Waste* **2023**, *1*, 775–805, doi:10.3390/waste1030046.
19. Herviyanti; Maulana, A.; Prasetyo, T.B.; Lita, A.L.; Harianti, M.; Monikasari, M. Characteristics of Glyphosate Adsorption with Biochar from Young Coconut Waste. *IOP Conf. Ser. Earth Environ. Sci.* **2023**, *1208*, doi:10.1088/1755-1315/1208/1/012050.
20. Dong, X.; Chu, Y.; Tong, Z.; Sun, M.; Meng, D.; Yi, X.; Gao, T.; Wang, M.; Duan, J. Mechanisms of Adsorption and Functionalization of Biochar for Pesticides: A Review. *Ecotoxicol. Environ. Saf.* **2024**, *272*, 116019, doi:10.1016/j.ecoenv.2024.116019.
21. Igliński, B.; Kujawski, W.; Kiełkowska, U. Pyrolysis of Waste Biomass: Technical and Process Achievements, and Future Development—A Review. *Energies* **2023**, *16*, 1829, doi:10.3390/en16041829.
22. Hermansah; Ermadani; Yulnafatmawita; Syarif, A.; Rusman, B. Optimizing Utilization of Palm Oil Mill Effluent and Its Influences on Nutrient Availability and Soil Organic Matter on Ultisols. *Int. J. Adv. Sci. Eng. Inf. Technol.*

- 2017**, 7, 257–262, doi:10.18517/ijaseit.7.1.1675.
23. Maulana, A.; Harianti, M.; Athiyya, S.; Prasetyo, T.B.; Monikasari, M.; Darfis, I.; Rezki, D.; Herviyanti, H. Biochar Quality During Slow Pyrolysis from Oil Palm Empty Fruit Bunches and Its Application as Soil Ameliorant. *Caraka Tani J. Sustain. Agric.* **2025**, 40, 84, doi:10.20961/carakatani.v40i1.93859.
 24. Pedroso-Rodriguez, I.; González-Sáez, L.Y.; Luis-Orozco, J.; Pérez-Martínez, L.; Vandecasteele, C.; Caneghem, J. Van Extraction Yield of Humic Substances from Organic Materials. *DYNA* **2022**, 89, 107–113, doi:10.15446/dyna.v89n223.101666.
 25. Alberti, G.; Amendola, V.; Pesavento, M.; Biesuz, R. Beyond the Synthesis of Novel Solid Phases: Review on Modelling of Sorption Phenomena. *Coord. Chem. Rev.* **2012**, 256, 28–45, doi:10.1016/j.ccr.2011.08.022.
 26. Foo, K.Y.; Hameed, B.H. Insights into the Modeling of Adsorption Isotherm Systems. *Chem. Eng. J.* **2010**, 156, 2–10, doi:10.1016/j.cej.2009.09.013.
 27. Hamdaoui, O.; Naffrechoux, E. Modeling of Adsorption Isotherms of Phenol and Chlorophenols onto Granular Activated Carbon. Part I. Two-Parameter Models and Equations Allowing Determination of Thermodynamic Parameters. *J. Hazard. Mater.* **2007**, 147, 381–394, doi:10.1016/j.jhazmat.2007.01.021.
 28. Ayawei, N.; Ebelegi, A.N.; Wankasi, D. Modelling and Interpretation of Adsorption Isotherms. *J. Chem.* **2017**, 2017, doi:10.1155/2017/3039817.
 29. Ayawei, N.; Angaye, S.S.; Wankasi, D.; Dikio, E.D. Synthesis, Characterization and Application of Mg/Al Layered Double Hydroxide for the Degradation of Congo Red in Aqueous Solution. *Open J. Phys. Chem.* **2015**, 05, 56–70, doi:10.4236/ojpc.2015.53007.
 30. Sen, K.; Chattoraj, S. A Comprehensive Review of Glyphosate Adsorption with Factors Influencing Mechanism: Kinetics, Isotherms, Thermodynamics Study. In *Intelligent Data-Centric Systems*; Bhattacharyya, S., Mondal, N.K., Platos, J., Snášel, V., Krömer, P.B.T.-I.E.D.M. for P.M., Eds.; Academic Press, 2021; pp. 93–125 ISBN 978-0-12-819671-7.
 31. Al-Ghouti, M.A.; Da'ana, D.A. Guidelines for the Use and Interpretation of Adsorption Isotherm Models: A Review. *J. Hazard. Mater.* **2020**, 393, 122383, doi:10.1016/j.jhazmat.2020.122383.
 32. Ott, E.-J.E.; Kucinski, T.M.; Dawson, J.N.; Freedman, M.A. Use of Transmission Electron Microscopy for Analysis of Aerosol Particles and Strategies for Imaging Fragile Particles. *Anal. Chem.* **2021**, 93, 11347–11356, doi:10.1021/acs.analchem.0c05225.
 33. Yaashikaa, P.R.; Kumar, P.S.; Varjani, S.; Saravanan, A. A Critical Review on the Biochar Production Techniques, Characterization, Stability and Applications for Circular Bioeconomy. *Biotechnol. Reports* **2020**, 28, e00570, doi:10.1016/j.btre.2020.e00570.
 34. Guo, H.; Li, X.; Zhang, J.; Huang, Z.; Urynowicz, M.A.; Liang, W. The Effect of NaOH Pretreatment on Coal Structure and Biomethane Production. *PLoS One* **2020**, 15, e0231623, doi:10.1371/journal.pone.0231623.
 35. Arnata, I.W.; Harsojuwono, B.A.; Hartiati, A.; Anggreni, A.A.M.D.; Sartika, D. Effect of Alkaline Concentration Treatments on the Chemical, Physical and Thermal Characteristics of Cellulose from Tapioca Solid Waste. *J. Fibers Polym. Compos.* **2022**, 1, 117–130, doi:10.55043/jfpc.v1i2.57.
 36. Rafatullah, M.; Ahmad, T.; Ghazali, A.; Sulaiman, O.; Danish, M.; Hashim, R. Oil Palm Biomass as a Precursor of Activated Carbons: A Review. *Crit. Rev. Environ. Sci. Technol.* **2013**, 43, 1117–1161, doi:10.1080/10934529.2011.627039.
 37. Elkhaleefa, A.; Ali, I.H.; Brima, E.I.; Shigidi, I.; Elhag, A.B.; Karama, B. Evaluation of the Adsorption Efficiency on the Removal of Lead(II) Ions from Aqueous Solutions Using Azadirachta Indica Leaves as an Adsorbent. *Processes* **2021**, 9, 559, doi:10.3390/pr9030559.
 38. Hong, T.; Yin, J.Y.; Nie, S.P.; Xie, M.Y. Applications of Infrared Spectroscopy in Polysaccharide Structural Analysis: Progress, Challenge and Perspective. *Food Chem. X* **2021**, 12, doi:10.1016/j.fochx.2021.100168.
 39. Tiwari, A.K.; Jha, S.; Singh, A.K.; Mishra, S.K.; Pathak, A.K.; Ojha, R.P.; Yadav, R.S.; Dikshit, A. Innovative Investigation of Zinc Oxide Nanoparticles Used in Dentistry. *Crystals* **2022**, 12, doi:10.3390/cryst12081063.
 40. Lin, H.; Xie, J.; Dong, Y.; Liu, J.; Meng, K.; Jin, Q. A Complete Review on the Surface Functional Groups in Pyrolyzed Biochar and Its Interaction Mechanism with Heavy Metal in Water. *J. Environ. Chem. Eng.* **2025**, 13, doi:10.1016/j.jece.2025.116681.
 41. Li, X.; Liu, H.; Liu, N.; Sun, Z.; Fu, S.; Zhan, X.; Yang, J.; Zhou, R.; Zhang, H.; Zhang, J.; et al. Pyrolysis Temperature

- Had Effects on the Physicochemical Properties of Biochar. *Plant, Soil Environ.* **2023**, *69*, 363–373, doi:10.17221/444/2022-PSE.
42. Zhao, B.; O'Connor, D.; Zhang, J.; Peng, T.; Shen, Z.; Tsang, D.C.W.; Hou, D. Effect of Pyrolysis Temperature, Heating Rate, and Residence Time on Rapeseed Stem Derived Biochar. *J. Clean. Prod.* **2018**, *174*, 977–987, doi:10.1016/j.jclepro.2017.11.013.
 43. Odoemelam, S.A.; Oji, E.O.; Eddy, N.O.; Garg, R.; Garg, R.; Islam, S.; Khan, M.A.; Khan, N.A.; Zahmatkesh, S. Zinc Oxide Nanoparticles Adsorb Emerging Pollutants (Glyphosate Pesticide) from Aqueous Solutions. *Environ. Monit. Assess.* **2023**, *195*, doi:10.1007/s10661-023-11255-0.
 44. Lyu, H.; Zhang, Q.; Shen, B. Application of Biochar and Its Composites in Catalysis. *Chemosphere* **2020**, *240*, doi:10.1016/j.chemosphere.2019.124842.
 45. Chilev, C.; Dicko, M.; Langlois, P.; Lamari, F. Modelling of Single-Gas Adsorption Isotherms. *Metals (Basel)* **2022**, *12*, 1698, doi:10.3390/met12101698.
 46. Alves, P.A. de T.; Munhoz-Garcia, G.V.; Nalin, D.; Mendes, K.F.; Tornisiello, V.L. Understanding the Complexities in Glyphosate and Ametryn Interactions: Soil Retention and Transformation as Influenced by Their Applications Alone and Mixture. *Crop Prot.* **2024**, *184*, doi:10.1016/j.cropro.2024.106803.
 47. Kimbi Yaah, V.B.; Ahmadi, S.; Quimbayo M, J.; Morales-Torres, S.; Ojala, S. Recent Technologies for Glyphosate Removal from Aqueous Environment: A Critical Review. *Environ. Res.* **2024**, *240*, 117477, doi:https://doi.org/10.1016/j.envres.2023.117477.
 48. Kalam, S.; Abu-Khamsin, S.A.; Kamal, M.S.; Patil, S. Surfactant Adsorption Isotherms: A Review. *ACS Omega* **2021**, *6*, 32342–32348, doi:10.1021/acsomega.1c04661.
 49. Herviyanti, H.; Maulana, A.; Rezki, D.; Yasin, S.; Prasetyo, T.B.; Mailiza, Y.M.; Darfis, I.; Dwipa, I. Identification of Insecticide Residues in Inceptisols at The Central of Horticultural Production, Banuhampu Agam West Sumatra. *IOP Conf. Ser. Earth Environ. Sci.* **2024**, *1297*, 012056, doi:10.1088/1755-1315/1297/1/012056.
 50. Silvani, L.; Cornelissen, G.; Hale, S.E. Sorption of α -, β -, γ - and δ -Hexachlorocyclohexane Isomers to Three Widely Different Biochars: Sorption Mechanisms and Application. *Chemosphere* **2019**, *219*, 1044–1051, doi:10.1016/j.chemosphere.2018.12.070.
 51. Sun, S.-J.; Wang, F.; He, Z.-W.; Tang, C.-C.; Zhou, A.-J.; Ren, Y.-X.; Li, Z.; Liu, W. Biochar Alleviates Inhibition Effects of Humic Acid on Anaerobic Digestion: Insights to Performances and Mechanisms. *Environ. Res.* **2024**, *259*, 119537, doi:https://doi.org/10.1016/j.envres.2024.119537.
 52. Fryda, L.; Visser, R. Biochar for Soil Improvement: Evaluation of Biochar from Gasification and Slow Pyrolysis. *Agriculture* **2015**, *5*, 1076–1115, doi:10.3390/agriculture5041076.
 53. Ukalska-Jaruga, A.; Bejger, R.; Smreczak, B.; Podlasiński, M. Sorption of Organic Contaminants by Stable Organic Matter Fraction in Soil. *Molecules* **2023**, *28*, 429, doi:10.3390/molecules28010429.
 54. Amalina, F.; Razak, A.S.A.; Krishnan, S.; Zularisam, A.W.; Nasrullah, M. A Comprehensive Assessment of the Method for Producing Biochar, Its Characterization, Stability, and Potential Applications in Regenerative Economic Sustainability – A Review. *Clean. Mater.* **2022**, *3*, 100045, doi:10.1016/j.clema.2022.100045.
 55. Wei, J.; Yan, L.; Zhang, Z.; Hu, B.; Gui, W.; Cui, Y. Carbon Nanotube/Chitosan Hydrogel for Adsorption of Acid Red 73 in Aqueous and Soil Environments. *BMC Chem.* **2023**, *17*, 104, doi:10.1186/s13065-023-01019-9.